Comparison of corrosion behaviour of copper and copper alloys in aqueous chloride solution

Gudic, Senka; Vrsalovic, Ladislav; Radeljic, Ana; Oguzie, Emanuel; Ivanic, Ivana; Kozuh, Stjepan; Gojic, Mirko

Source / Izvornik: **Chemical Industry and Chemical Engineering Quarterly, 2021, 27, 383 - 394**

Journal article, Published version
Rad u časopisu, Objavljena verzija rada (izdavačev PDF)

https://doi.org/10.2298/ciceq200701007g

Permanent link / Trajna poveznica: https://urn.nsk.hr/urn:nbn:hr:115:790790

CI&CEQ
Chemical Industry & Chemical Engineering Quarterly

Available on line at
Association of the Chemical Engineers of Serbia *AChE*
www.ache.org.rs/CICEQ

Chem. Ind. Chem. Eng. Q. 27 (4) 383–394 (2021) CI&CEQ

SENKA GUDIĆ[1]
LADISLAV VRSALOVIĆ[1]
ANA RADELJIĆ[1]
EMEKA EMANUEL OGUZIE[2]
IVANA IVANIĆ[3]
STJEPAN KOŽUH[3]
MIRKO GOJIĆ[3]

[1]University of Split, Faculty of Chemistry and Technology, Department of Electrochemistry and Materials Protection, Split, Croatia
[2]Federal University of Technology Owerri, Africa Centre of Excellence in Future Energies and Electrochemical Systems (ACE-FUELS), Owerri, Nigeria
[3]University of Zagreb, Faculty of Metallurgy, Sisak, Croatia

SCIENTIFIC PAPER

UDC 669.35:620.193:66.09

COMPARISON OF CORROSION BEHAVIOR OF COPPER AND COPPER ALLOYS IN AQUEOUS CHLORIDE SOLUTION

Article Highlights

- A detailed comparison of the corrosion behavior of Cu and 4 Cu alloys in NaCl solution was given
- EIS results indicate that sample resistance is the consequence of the formation of a barrier layer
- Alloying elements have a positive effect on copper passivation and surface film properties
- SEM/EDS analyses have shown that Cu alloys all had thicker and more protective barrier layers

Abstract

A comparative corrosion study of Cu and Cu-Al, Cu-Al-Ni, Cu-Al-Mn and Cu-Al-Mn-Ni in 0.5 mol dm^{-3} NaCl solution was performed using an open circuit potential, potentiodynamic polarization and electrochemical impedance spectroscopy measurements (EIS). Scanning electron microscopy/energy-dispersive X-ray spectroscopy (SEM/EDS) analysis was used to evaluate corrosive damage on the sample surface after polarization measurements. The reported results suggest that the alloying elements have reduced cathodic and anodic current densities in the Tafel region, increased anodic currents at higher anodic potentials, and slightly displaced corrosion potential towards more positive values. Overall, impedance increased in the following order: Cu < Cu-Al < Cu-Al-Ni < Cu-Al-Mn < Cu-Al-Mn-Ni. This indicates that Cu alloys possess better corrosion resistance. SEM and EDS analysis after polarization measurements showed uniform dissolution of pure Cu, as well as the presence of a surface oxide layer, consisting of a mixture of the corresponding alloying elements, on all investigated alloys. Aggressive anodic polarization severely damaged the barrier layers on the Cu alloy specimens.

Keywords: copper alloys, corrosion, electrochemical methods, polarization, shape memory alloys, SEM/EDS.

Copper and its alloys have significant practical applications due to their high electrical and thermal conductivity, workability, and good corrosion resistance in a variety of environments. These materials have been used in the production of condenser tubes for ships, heat exchanger tubing materials in power plants, and other industries, such as pipeline networks, valves, pumps, fittings, etc. [1-5]. Cu-Al alloys, also known as aluminium bronzes, with aluminium contents up to 14 wt.%, exhibit an excellent combination of strength and corrosion resistance, making them one of today's most important engineering materials for highly stressed components in corrosive environments. Stress-corrosion fatigue resistance of Cu-Al alloys exceeds that of austenitic stainless steels. Additionally, they can be machined or ground and are readily weldable [4,6,7]. Upon addition of Ni or/and Mn to Cu-Al alloys, new alloys can be produced that exhibit specific properties, including Cu shape memory alloys (SMAs). An SMA remembers its original shape, returning to its pre-deformed shape upon heating [8]. At high temperatures, SMAs exist in

Correspondence: L. Vrsalović, University of Split, Faculty of Chemistry and Technology, Ruđera Boškovića 35, 21000 Split, Croatia.
E-mail: ladislav@ktf-split.hr
Paper received: 1 July, 2020
Paper revised: 3 December, 2020
Paper accepted: 1 March, 2021

https://doi.org/10.2298/CICEQ200701007G

an austenite phase, and upon cooling below the transformation temperature, the austenite transforms to a thermoelastic martensite. Cu-Al-Ni and Cu-Al-Mn SMAs have been extensively investigated and have found practical usage in actuator and sensor manufacturing, electronics, computers parts, automotive and aircraft industries, robotics, and civil engineering industry, etc. [9-13].

Due to the wide application of Cu and Cu alloys, these materials come into contact with various aggressive media that can significantly affect their durability and change their properties, so understanding the mechanisms of corrosion in Cu alloys is important for many contemporary applications, including microelectronics, robotics, aerospace industry, or as canister materials for nuclear waste storage. In these cases, even extremely small corrosion rates may be detrimental, due either to the small amount of material present or the long lifetimes required.

The corrosion behaviour of copper and its alloys strongly depends on the electrolyte composition in contact with the metal surface, as well as elements present in the alloys. Most published results have been obtained in chloride-containing media, as chlorides are one of the most common corrosive agents in nature and copper alloys are considered promising materials for marine applications [14-18].

Investigations of anodic Cu dissolution have shown that in the absence of complexing substances in the electrolyte (*i.e.*, Cl^-, NH_3, etc.), dissolution takes place in two stages [14]:

$$Cu \leftrightarrow Cu^+ + e^- \quad \text{(fast reaction)} \tag{1}$$

$$Cu^+ \leftrightarrow Cu^{2+} + e^- \quad \text{(slow reaction)} \tag{2}$$

In the presence of complexing Cl^-, consideration should be given to the possibility of $CuCl_2^-$ complex formation. In the region near the corrosion potential and at Cl^- concentrations less than 1 mol dm^{-3}, the Cu dissolution mechanism takes place in two stages. The first stage is CuCl formation, which is adsorbed on the surface of the electrode, according to reaction (3) [15,19,20]:

$$Cu + Cl^- \leftrightarrow CuCl_{ads} + e^- \tag{3}$$

Upon reaction with another Cl^-, the adsorbed compound on the electrode surface is dissolved, forming a soluble $CuCl_2^-$ complex (reaction (4)). Further, the $CuCl_2^-$ complex on the electrode surface is subject to a hydrolysis reaction, which leads to the formation of Cu_2O (reaction (5)) [15,19,20]:

$$CuCl + Cl^- \leftrightarrow CuCl_2^- \tag{4}$$

$$2CuCl_2^- + H_2O \rightarrow Cu_2O + 4Cl^- + 2H^+ \tag{5}$$

$CuCl_2^-$ diffuses from the surface to the mass of the solution, a slow process in the Cu dissolution reaction. As a result of these reactions, layers of corrosion products are formed on the surface (mostly as oxide, hydroxide or chloride), which can slow the rate of anodic dissolution, as well as the cathodic reaction. This can be represented by equation (6) in neutral aerated solution [15,16,20]:

$$O_2 + 2H_2O + 4e^- \rightarrow 4OH^- \tag{6}$$

Aluminium is one attractive alloying element used to enhance the corrosion resistance of copper-based alloys. Addition of aluminium to a Cu-based alloy increases its corrosion resistance due to the formation of a protective alumina (Al_2O_3) layer, along with Cu_2O, which builds up quickly on the surface exposed to the corrosive environment. The formation of these stable passive layers on Cu-Al alloys is mainly due to the higher affinity of aluminium towards oxygen than copper in salt solution and considerable stability of Al_2O_3 over Cu_2O [7,21,22].

Cu-Ni alloys have been widely studied in NaCl solutions, but published results regarding the dissolution process are contradictory. Some authors pointed out that selective removal of nickel is predominant [23,24], while others have suggested that the main process is the de-alloying of copper [25]. Investigations on corrosion resistance of Cu-Ni alloys in chloride solution, performed by Milošev and Metikoš-Huković [26,27], have indicated a passive layer on Cu-$_x$Ni alloys (x in range 10-40 wt.%), consisting of an outer $CuO/Cu(OH)_2$ layer overlaying a Cu_2O barrier layer with incorporated nickel cations. This incurporation takes place because of the defective inner Cu_2O layer structure, which can accept large amounts of foreign ions, such as nickel or iron. Recent studies have confirmed that the presence of nickel is important in the passivation of Cu-Ni alloys because of its incorporation into the oxide layer, reducing the number of cation vacancies in Cu(I) oxide formed on the corroded alloy surface [22,28-30]. Incorporation of nickel and iron (in Cu-Ni-Fe alloys) leads to a decrease in both ionic and electronic conductivities of the oxide film [26,31].

Nady *et al.* have shown that an increase in nickel content decreases the corrosion rate of Cu-Al-Ni ternary alloys in chloride solutions [30]. However, Badawy *et al.* have reported that the corrosion rate of Cu-Al-Ni SMAs increased with increasing Ni content. They explained this behaviour by the fact that, according to the Pourbaix diagrams, Cu and Al form

the most stable species, but Ni is active in the same conditions. Thus, the increase in i_{corr} for alloys with higher Ni content was interpreted by the dissolution of Ni with the formation of Ni^{2+} [31].

The addition of Mn in small amounts to the Cu-Al alloys influences alloy microstructure, *i.e.* reduces the crystal grain size. Specifically, Mn diffuses easily and rapidly disperses through the alloy mass, accumulating on the grain boundaries, thus preventing further grain growth [21,32]. Studies have shown that such microstructure refining, with the improvement of mechanical properties also increases alloy corrosion resistance as this fine microstructure positively affects the compactness and stability of the passive oxide film [21].

Also, the addition of some other alloying elements, like beryllium in Cu-Al alloys, leads to increased resistivity towards intergranular corrosion due to the diffusion of beryllium atoms into grain boundaries, which, in turn, deactivates the grain boundaries [33]. Beneficial influence on corrosion resistance has been achieved by alloying Cu-Al-Ni alloys with Ti and Ag nanoparticles [21,34]. Decreasing grain size as a result of Ti addition (similar to Mn addition) leads to the formation of a passivation film, resulting in an increase of its resistance to pit nucleation. Moreover, the presence of Ti and Mn in the passivation film (in a form of Al_2TiO_5, TiO_2, $TiCl_2$, $CuMnO_2$ and Mn_2O_3) protects the SMAs from the aggressive action of Cl^- better than corrosion layers in the base alloy, while the presence of Ag nanoparticles leads to formation of the corrosion products silver chloride, cuprous oxide, aluminium oxide/hydroxide, and silver oxide, which act as protective layers and improve the corrosion resistance of Cu-Al-Ni-Ag SMA. In this paper, results of a comparative electrochemical behaviour study of pure copper and Cu-Al, Cu-Al-Ni, Cu-Al-Mn, and Cu-Al-Mn-Ni alloys in 0.5 mol dm^{-3} NaCl solution are presented.

EXPERIMENTAL

Chemical compositions of materials used in this investigation are given in Table 1.

The working electrodes were prepared by cutting appropriate metal rods to small cylindrical specimens, which were then soldered to isolated Cu wires for good electrical contact. Electrodes were isolated with Polirepar S protective mass so that only a circular cross-section (0.5 cm^2) was exposed to the electrolyte. Prior to every experiment, the electrode was ground and polished with successive wet SiC emery papers (from 400 to 1500) using a Metkon Forcipol 1V grinder and polisher. Samples were polished with Al_2O_3 polishing paste (particle size 0.05 μm), ultrasonically degreased in ethanol, rinsed with deionized water, and immersed in electrolyte solution. Measurements were carried out in a water-jacketed glass electrochemical cell equipped with platinum foil as a counter electrode and a saturated calomel electrode (SCE) as the reference electrode. The SCE was connected to the cell via a Luggin capillary, and the electrochemical cell was connected to a Huber Kiss heating and cooling circulator at 20 °C. Measurements were performed in 0.5 mol dm^{-3} NaCl solution, prepared by dissolution of pure NaCl salt, obtained by Kemika Zagreb, in a measuring flask with deionized water.

A potentiostat/galvanostat (Princeton Applied Research; PAR; M273A) connected with a PAR M5210 lock-in amplifier was employed for electrochemical measurements. Open circuit potential measurements (E_{OC}) were carried out in 60-min time periods, and potentiodynamic polarization tests were conducted in the potential region from −0.250 V *vs.* E_{OC} to 1.1 V with a scanning rate of 0.5 mV s^{-1}. Impedance spectra were recorded at E_{OC} in the frequency range of 50 kHz to 30 mHz with five points per decade and an AC voltage amplitude of ±10 mV. The experimental impedance spectra were analysed and interpreted on the basics of the equivalent circuit program of Boukamp [35].

For every investigated sample, the same experimental procedures were applied for comparison of obtained results. The prepared electrode was immersed in electrolyte, and immediately thereafter E_{OC} measurements were performed. Afterwards, EIS measurements were conducted with the same electrode at E_{OC}, and at the end, potentiodynamic polarization

Table 1. Chemical compositions of investigated samples

Material	Composition, wt.%
Cu	99.90
Cu-Al	90.90 Cu, 9.10 Al
Cu-Al-Ni	84.67 Cu, 11.29 Al, 4.05 Ni
Cu-Al-Mn	82.30 Cu, 8.30 Al, 9.40 Mn
Cu-Al-Mn-Ni	82.00 Cu, 13.00 Al, 2.50 Mn, 2.50 Ni

was applied as the last destructive electrochemical method.

After potentiodynamic experiments, electrode surfaces were ultrasonically cleaned in deionised water to remove loose corrosion products, dried in a desiccator, and, then, analyzed by a scanning electron microscope (SEM; Tescan Vega TS5136LS). Quantitative analysis of elements on the electrode surface was determined by energy dispersive spectroscopy (EDS).

RESULTS AND DISCUSSION

Open circuit potential measurements

Figure 1 illustrates the E_{OC} decay for all studied electrodes in 0.5 mol dm^{-3} NaCl solution. The change of E_{OC} is the consequence of changes that occur due to non-equilibrium electrochemical processes at the electrode/solution interface. Specifically, the established E_{OC} value depends on the conditions of the measurement being performed, the composition and state of the surface of the examined metal sample, the characteristics of the electrolyte solution, and the exposure time of the metal sample to electrolyte. After some time, the value of the E_{OC} will be set around a certain equilibrium value.

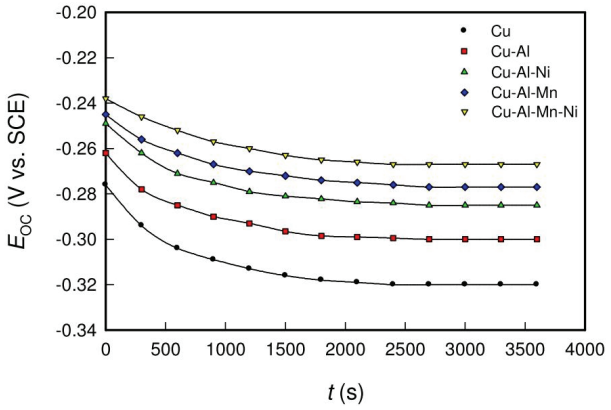

Figure 1. Open circuit potential vs. time curves for investigated samples in 0.5 mol dm^{-3} NaCl solution.

From Figure 1, all tested samples show similar trends in potential changes over time; a steady negative shift of E_{OC} is observed, after which stable values are established. The same trend was observed for all investigated samples: E_{OC} values shift towards more negative values over time. Similar behavior was observed for Cu and Cu alloys in NaCl solutions in the literature [5,7,16,18,31,36]. Alfantasi *et al.* [18] attributed this behaviour to breakdown of the oxide film, exposing underlying Cu alloy surfaces to the electrolyte and can lead to the dealloying and simultaneous dissolution of Cu and Al or Zn in Cu-Al and Cu-Zn alloys. In the case of Cu-Ni alloys, dealloying is more difficult due to the small differences between the Cu and Ni standard reversible potentials.

Figure 1 shows that the steady state potential was achieved within 40 min of electrode immersion in the solution. Values of E_{OC} for all the Cu alloys were more positive than Cu, as follows: Cu < Cu-Al < Cu-Al-Ni < Cu-Al-Mn < Cu-Al-Mn-Ni. This suggests that Cu presents a more active surface than all Cu alloys.

Potentiodynamic polarization measurements

Polarization experiments enabled the effects of alloying elements on the anodic and cathodic partial reactions of Cu to be assessed over a wide range of potentials in the NaCl environment. The anodic dissolution of Cu and Cu alloys in chloride-containing solutions has been extensively reported in the literature [15-27,31,36-41], revealing that the mechanism of anodic polarization is mostly controlled by mass-transport of chlorides. Generally, Cu is considered to be uniformly dissolved throughout the surface, creating a layer of corrosion products composed mainly of CuCl (which easily converts into soluble $CuCl_2^-$ complexes) and Cu_2O. Figure 2 shows the potentiodynamic polarization curve for the Cu electrode in 0.5 mol dm^{-3} NaCl solution. Consistent with previous reports for Cu in chloride media [15,34,38], the anodic polarization curve consists of three regions with distinctive features: a Tafel region, a region where the current peaks and then drops to a minimum, and a region of high anodic potentials, with an increase in anodic current density due to the corrosion product film breakdown and continuation of Cu dissolution with formation of Cu(II) species.

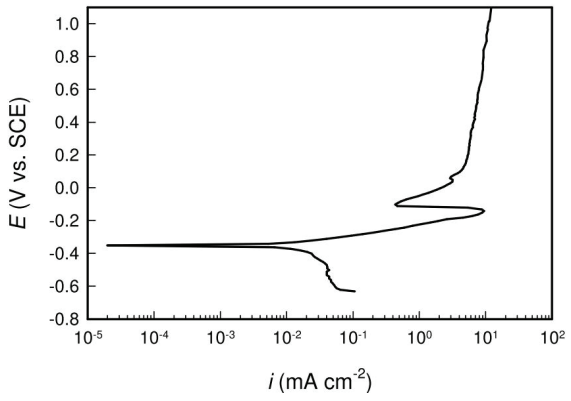

Figure 2. Potentiodynamic polarization curves for Cu in 0.5 mol dm^{-3} NaCl solution.

The potentiodynamic polarization curves of the Cu and Cu-alloy specimens in 0.5 mol dm^{-3} NaCl

solution are shown in Figure 3. The plots show clearly that all Cu alloys display similar polarization features to pure Cu, with distinct active-pseudo passive transitions in the studied potential range. The five anodic curves exhibited typical Tafel-type active regions, where the logarithm of corrosion current density (log *i*) was proportional to the potential (*E*) with similar anodic slopes. Determined values of anodic Tafel slopes were close to the 60 mV/dec for Cu and Cu alloys. This implies that anodic behavior of these Cu alloys in chloride solutions is dominated by the diffusion rate of soluble cuprous chloride ion complexes ($CuCl_2^-$), formed during the dissolution of copper and its alloys and confirmed in the literature [18,37,42]. When Al is present on the electrode surface, one corrosion product will be aluminium chloride salt, which can be dissolved as aluminium chloride ions, in addition to the dissolution of copper as a copper chloride complex ion [43]. In spite of Al dissolution, the apparent Tafel slopes of Cu-Al and other investigated alloys have similar values to pure copper, suggesting that the same rate-determining step is operating for both pure copper and copper-based alloys [37,42].

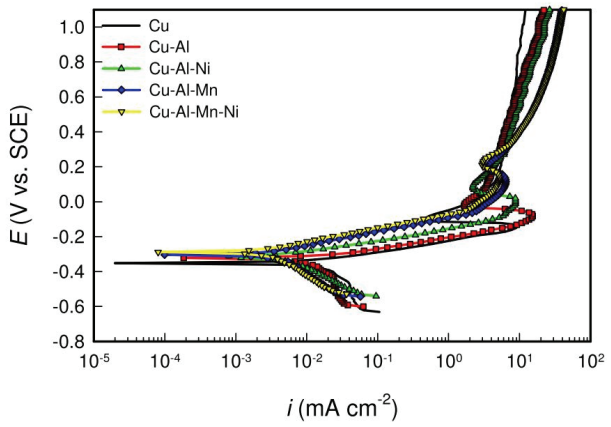

Figure 3. Potentiodynamic polarization curves of investigated samples in 0.5 mol dm^{-3} NaCl solution.

This means that the alloying elements did not notably modify the copper dissolution mechanism in the anodic Tafel region. However, the presence of alloying elements caused some changes in the polarization behavior of the Cu electrode, which reduces the cathodic and anodic current densities within the Tafel region, increasing the anodic currents at higher potentials and slightly displacing the corrosion potential towards more positive (noble) values. At higher anodic potentials outside the Tafel region, all anodic curves reached maximum values at different anodic potentials. Afterwards, the anodic current densities dropped due to slower anodic dissolution through the formed surface film of corrosion products. The film's coverage on the electrode surface temporarily delays the current density increase and then continues further as the electrode potential becomes more positive. Breakdown of surface films at higher anodic potentials lead to intensive dissolution, and anodic current density increases.

Corrosion parameters, such as corrosion potential (E_{corr}), values of anodic and cathodic Tafel slopes (b_a and b_c), and corrosion current density (i_{corr}), are determined by polarization curve analysis, and the obtained values for each sample are shown in Table 2. Polarization resistance (R_p) values were calculated using the Stern-Geary equation [44] and are also shown in Table 2.

Interestingly, the observed variations in the Cu alloys' behaviour are concomitant with the increase in amounts of alloying elements and decrease in Cu content, as reflected in Table 1. Table 2 shows E_{corr} values of the Cu alloys to be nobler than pure Cu, and the trend coincides exactly with the trend of E_{OC} values in Figure 1. The anodic current densities in the Tafel region (as well as i_{corr} values from Table 2) are lower in Cu alloys compared to pure Cu, as follows: Cu > Cu-Al > Cu-Al-Ni > Cu-Al-Mn > Cu-Al-Mn-Ni. The transition from peak to minimum current occurred at increasingly higher potentials for the different Cu alloy specimens, in concise agreement with the trend of E_{corr}. However, at the high potential region, the trend of current density reverses and the anodic current densities of the Cu alloys surpass pure Cu as follows: Cu < Cu-Al < Cu-Al-Ni < Cu-Al-Mn < Cu-Al-Mn-Ni. Similar behaviour was reported by Sun [39] for Cu-based metal matrix composites, attributed to an increase in the galvanic current contribution for the alloy specimens at high potentials. Moreover, the reduced Cu content in the alloys means that contribut-

Table 2. Corrosion parameters for investigated samples obtained from polarization measurements

Sample	E_{corr} (mV)	b_a (mV dec^{-1})	b_c (mV dec^{-1})	i_{corr} (μA cm^{-2})	R_p (kΩ cm^2)
Cu	-351.01	65.77	242.31	13.95	1.61
Cu-Al	-324.44	65.63	220.50	6.56	3.89
Cu-Al-Ni	-316.42	69.01	211.12	5.17	4.37
Cu-Al-Mn	-300.59	83.34	241.43	3.48	7.74
Cu-Al-Ni-Mn	-290.40	81.27	250.68	2.83	9.43

ions from the expected polarization behavior of Cu would be reduced.

Impedance measurements

Impedance measurements on Cu and Cu alloys were performed at the E_{OC} after 60 min of electrode stabilization in NaCl solution. The obtained results are presented in Nyquist and Bode complex planes (Figure 4).

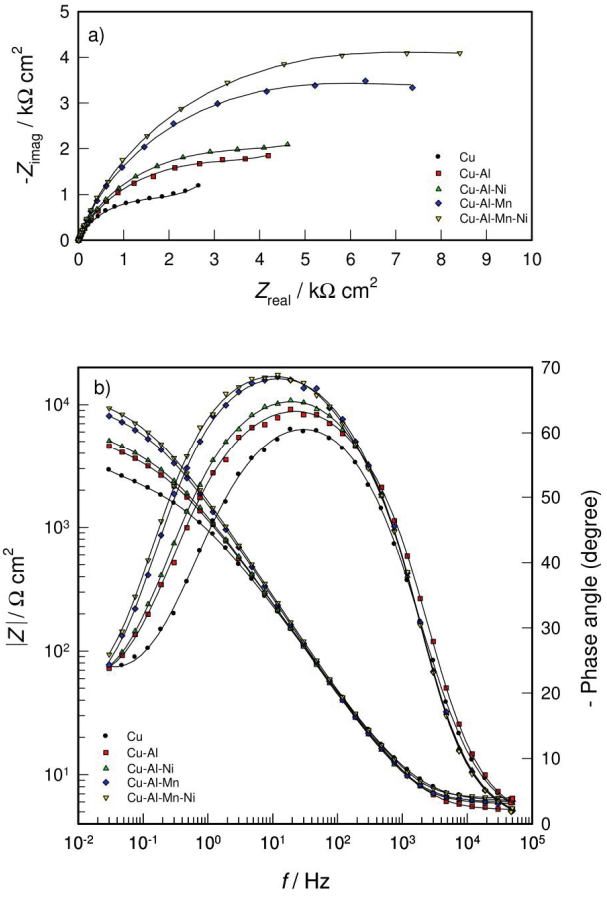

Figure 4. Nyquist (a) and Bode (b) plots of investigated samples in 0.5 mol dm^{-3} NaCl solution.

The Nyquist plots for all examined samples show evidence of two time constants that partially overlap. The Bode plots at medium frequencies with negative slopes and phase angles, approaching -70°, confirm the capacitive behavior of the examined systems, suggesting that a corrosion product surface film is formed on all tested materials. Similar observations have been reported in the literature [28,45-50]. All the tested samples show similar responses in Nyquist and Bode plots at E_{OC}, implying that the processes at the metal/solution interface for each system are similar. However, the overall impedance increased as follows, Cu < Cu-Al < Cu-Al-Ni < Cu-Al-Mn < Cu-Al-Mn-Ni, indicating that the Cu alloys possess better corrosion resistance.

In mathematical analysis of impedance diagrams, a constant phase element, CPE, is often used instead of an "ideal" capacitor to compensate for the depressed nature of the capacitive loops. The impedance, Z_{CPE}, of CPE is described by Eq. (7) [50]:

$$Z_{KFE} = \left[Q(jw)^n \right]^{-1} \tag{7}$$

with $-1 \leq n \leq 1$ and $j = \sqrt{-1}$, while Q is a frequency independent constant, defined as pure capacitance for $n = 1$, resistance for $n = 0$, and inductance for $n = -1$. Diffusion processes are characterised by the value of $n = 0.5$.

The equivalent circuit proposed to fit the experimental data is shown in Figure 5.

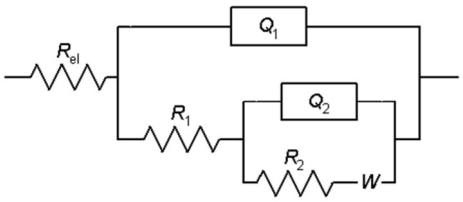

Figure 5. Proposed equivalent circuit for modelling the impedance data.

The CPEs, Q_1 and Q_2, represent the capacitances C_1 and C_2. The first time constant, Q_1R_1, observed in the high frequency region results from the fast charge transfer process in the metal dissolution reaction. In this case, R_1 represents the charge transfer resistance, and Q_1 replaces the capacitance of the electrical double layer. To account for the surface corrosion product layer and diffusion process in the low frequency region, additional equivalent circuit parameters were introduced, such as R_2 for the surface layer resistance, Q_2 for the CPE element of the surface layer (Q_2 replaces the capacitance of surface layer), and Warburg impedance, W, for the diffusion process. The calculated equivalent circuit parameters for all tested alloys are presented in Table 3.

The double layer capacitance (Q_1), surface layer capacitance (Q_2), and diffusion coefficient (W) decrease, while the charge transfer resistance (R_1) and surface layer resistance (R_2) increase in the following order: Cu < Cu-Al < Cu-Al-Ni < Cu-Al-Mn < Cu-Al-Mn-Ni.

Indeed, the impedance response of the Cu alloy specimens should be controlled largely by Cu dissolution, since Cu is the main constituent of these alloys and is also highly active in chloride-containing solutions. Furthermore, according to the plate capacitor

Table 3. Equivalent circuit parameters for investigated samples

Sample	$Q_1\times10^6$ (Ω^{-1} s^{n}cm^{-2})	n_1	R_1 (Ω cm^2)	$Q_2\times10^6$ (Ω^{-1} s^{n}cm^{-2})	n_2	R_2 (kΩ cm^2)	$W\times10^3$ (Ω^{-1} s^{n}cm^{-2})
Cu	55.78	0.86	19.92	177.14	0.63	2.38	1.76
Cu-Al	49.01	0.88	23.17	160.36	0.65	4.56	1.51
Cu-Al-Ni	49.89	0.90	25.68	150.92	0.66	5.19	1.43
Cu-Al-Mn	42.22	0.91	29.15	106.72	0.71	8.65	1.12
Cu-Al-Ni-Mn	40.15	0.91	33.26	98.49	0.72	10.17	0.97

model, the surface film capacitance is inversely proportional to thickness, d (according to $C = \varepsilon_o\varepsilon/d$, ε_o is the permittivity of vacuum and ε the relative permittivity of the film). Therefore, the reduction of the surface layer capacitance element, *i.e.*, parameter Q_2 (from 177.14 for Cu to 98.49 Ω^{-1} s^n cm^{-2} for the Cu-Al-Mn-Ni alloy), corresponds to an increase in the thickness of the surface layer in the same order. This direction of changes points to the fact that Al, Ni, and Mn reinforce the corrosion product layer at E_{corr} and effectively prevent alloy corrosion.

SEM/EDS analysis

The observed similarities in the electrochemical corrosion behavior of the studied Cu and Cu alloys means that the alloying elements did not modify the dissolution mechanism of Cu. Indeed, the impedance data show that the main effect of the alloying elements was to reinforce and thicken the corrosion product (barrier) layer and make it more protective; hence, the corrosion resistance of the tested samples increased in the following order: Cu < Cu-Al < Cu-Al-Ni < Cu-Al-Mn < Cu-Al-Mn-Ni. Polarization experiments, however, revealed that the protective effect of the corrosion product layers on the Cu alloy surfaces failed at high anodic potentials. Such failure implies that the protective barrier layer might have been compromised at high anodic potentials. To further probe these observations, SEM and EDS surface investigations were undertaken. Ultrasonic cleaning of the Cu surface in deionized water after potentiodynamic polarization measurements removed loose and porous corrosion products, enabling clear SEM visualization of the post-polarization corrosion morphology of Cu and Cu alloys.

The SEM/EDS image of the corroded Cu and SEM images of corroded Cu alloy specimens after potentiodynamic polarization are presented in Figures 6 and 7, respectively.

Two distinct features are observed from the SEM images in Figures 6 and 7. Firstly, the Cu alloy specimens all have thicker and more protective barrier layers than pure Cu, in agreement with the impedance data. Secondly, the aggressive anodic polarization at high potentials caused a breakdown of the corrosion product barrier layers on the alloy surfaces, consistent with polarization data. Indeed, EDS analysis of the corroded Cu surface (Figure 6) showed a high surface concentration of Cu, almost completely free of corrosion products (with only a minimal presence chlorine and oxygen). Cu is generally thought to dissolve in chloride solution according to reactions 1-5 (shown in the introduction), creating a layer of corrosive products composed mainly of CuCl, which easily passes into the soluble $CuCl_2^-$ complex, and Cu_2O. The corrosion product layer has poor protective

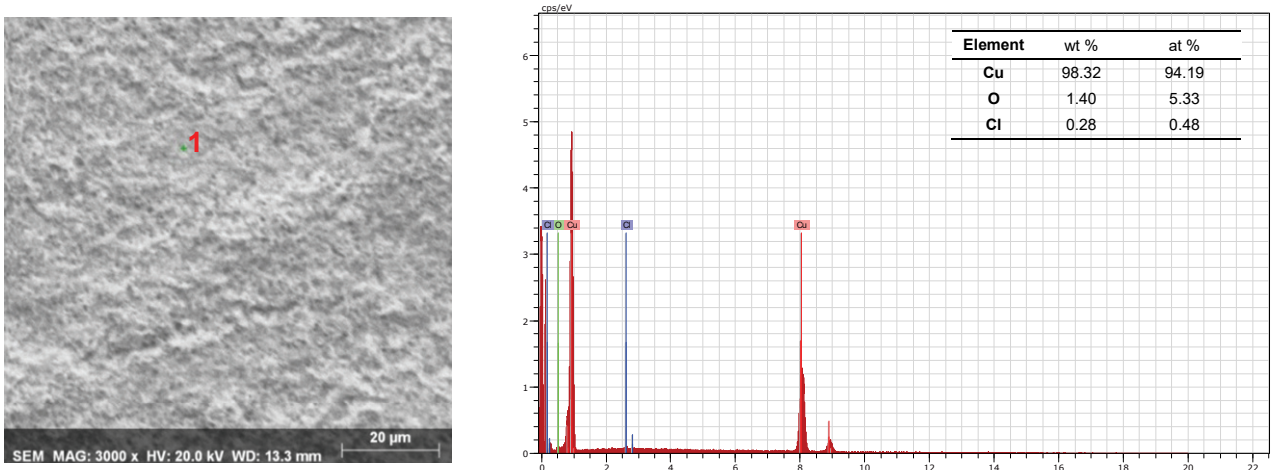

Figure 6. SEM/EDS analysis of the corroded Cu electrode surface (magnification 3000X).

properties; it is porous and does not prevent further diffusion of $CuCl_2^-$ from the electrode surface to the electrolyte solution. Ultrasonic cleaning of the Cu surface in deionized water after the polarization measurements completely removed the porous layer of corrosion products. This was confirmed by SEM/EDS surface investigations, showing rough irregular surfaces caused by corrosion dissolution and a high surface concentration of Cu, almost completely free of corrosion products, *i.e.*, the presence of chlorine and oxygen was confirmed in very small percentages (Figure 6).

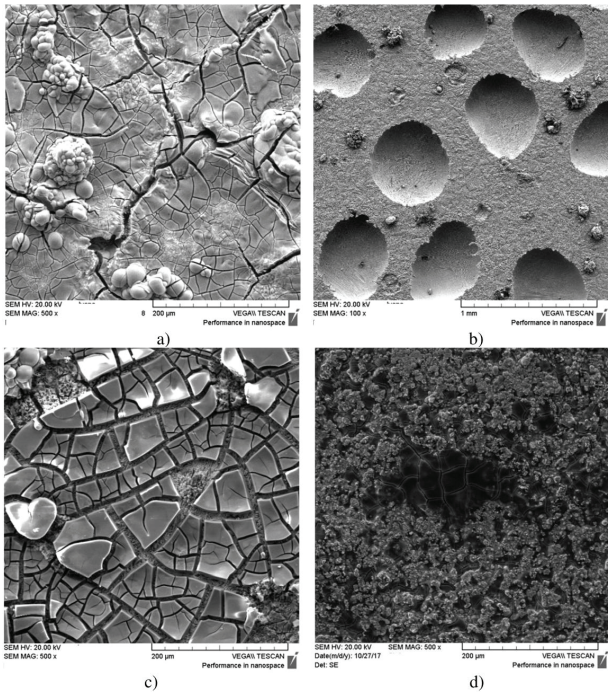

Figure 7. SEM images of corroded electrode surfaces: a) Cu-Al (magnification 500X), b) Cu-Al-Ni (magnification 100X), c) Cu-Al-Mn (magnification 500X), and d) Cu-Al-Mn-Ni (magnification 500X).

For more efficient characterization of the chemical composition of corroded alloy surfaces, EDS analyses were carried out at different locations - the intact remnant of the barrier layer and the bare metal surface beneath the cracked portions of the corrosion product (as shown in Figure 8 and presented in Table 4 for all investigated alloys).

The corrosion surface of Cu-Al alloys may be composed of different products (Cu_2O, $CuCl_2$, Al_2O_3, $AlCl_4$, etc.) [7]. Al reacts with Cl^- and forms $AlCl_4^-$, according to reaction (8). Since the chlorides are thermodynamically unstable in the presence of oxygen, chlorides react with water and form an Al_2O_3 oxide layer (reaction (9)). The formation of Al_2O_3, as an additional passivation process, protects the sample surface [7]:

$$Al + 4Cl^- \rightarrow AlCl_4^- + 3e^- \quad (8)$$

$$2AlCl_4^- + 3H_2O \rightarrow Al_2O_3 + 8Cl^- + 6H^+ \quad (9)$$

The high corrosion resistance of Cu-Al and other multicomponent alloys containing Al is primarily due to the presence of a bi-layered, structured corrosion product, with a protective inner thin compact layer, comprising mainly Cu_2O and Al_2O_3, and an outer porous layer enriched with copper, mainly in the form of Cu_2O [30,31,51,52].

SEM/EDS surface analysis was conducted after potentiodynamic polarization of the sample (Figures 6b and 8a). SEM images show the Al_2O_3 layer, which cracked because of the aggressive anodic polarization, along with aggregates of the porous layer that are held tighter on the surface and are not removed by ultrasonic cleaning (Al_2O_3 porous layer containing Cu_2O and CuCl). EDS analysis (Figure 8b and Table 4) indicated a high surface concentration of Al and O (position 1) and porous layer aggregates (position 2) with O and Al, as well as minor percentages of Cu and Cl. Furthermore, under the oxide layer, *i.e.*, in its cracks, a high concentration of Cu was confirmed, while Cl was practically absent (position 3).

SEM images of the Cu-Al-Ni alloy shows a rather thick and loose corrosion product layer, with pit-like cavities spread around, similar to previous investigations [53]. The EDS analysis at positions outside and inside the cavities indicates high percentages of Al, O and Ni, in addition to Cu. The higher corrosion resistance of Cu-Al-Ni alloys compared to Cu-Al, according to literature, is attributed to the incorporation of Ni^{2+} into a Cu_2O film, which consumes cation vacancies [54,55]. According to the "point defect" model [54,55] of movable cationic vacancies (V_{Cu}-(ox)), vacant cationic sites are formed by dissolving the Cu_2O surface layer:

$$Cu_{Cu}(ox) \rightarrow Cu^+(aq) + V_{Cu}\text{-}(ox) \quad (11)$$

A neutral complex forms by "jumping" Ni in the vacant cationic site on the surface of the alloy, according to reaction (12):

$$Ni_{Ni}(m) + 2V_{Cu}\text{-}(ox) \rightarrow \left[Ni_{Cu}(V_{Cu})_2\right] + 2e^- \quad (12)$$

The formation of this complex affects the reduction of ionic conductivity of the barrier oxide layer, which ultimately increases corrosion resistance of the alloy.

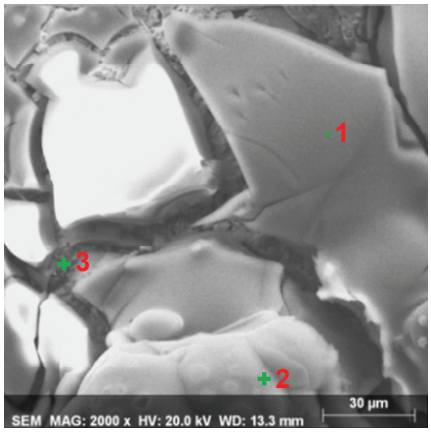

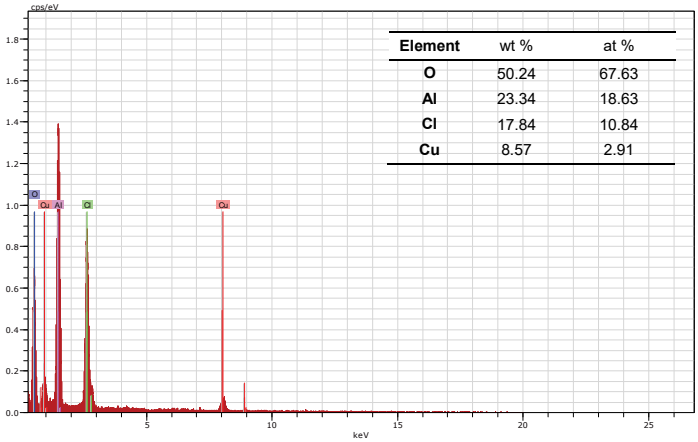

Element	wt %	at %
O	50.24	67.63
Al	23.34	18.63
Cl	17.84	10.84
Cu	8.57	2.91

a)

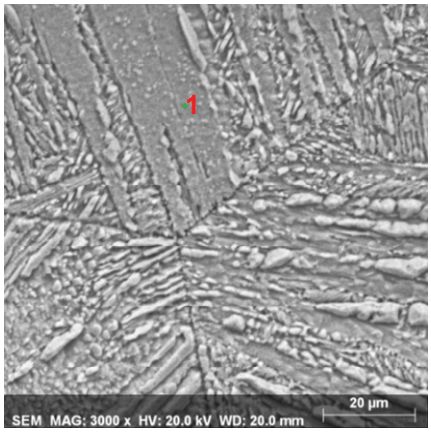

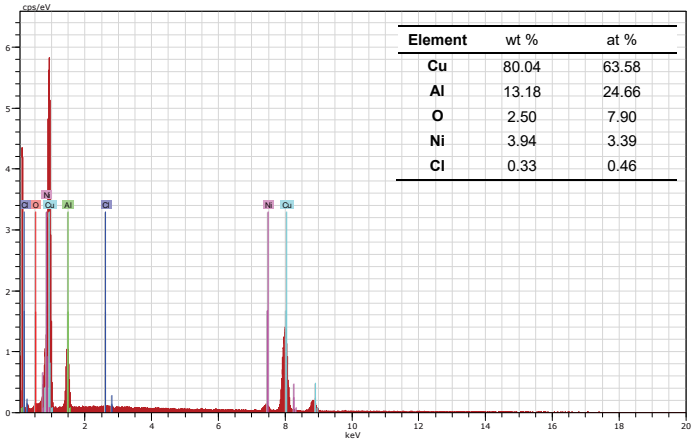

Element	wt %	at %
Cu	80.04	63.58
Al	13.18	24.66
O	2.50	7.90
Ni	3.94	3.39
Cl	0.33	0.46

b)

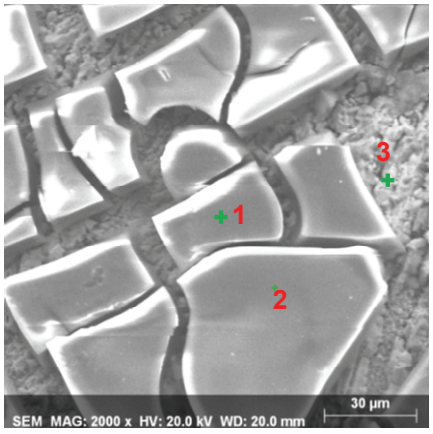

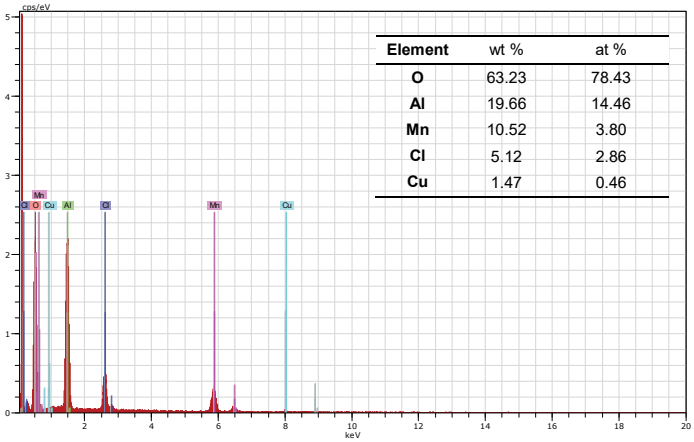

Element	wt %	at %
O	63.23	78.43
Al	19.66	14.46
Mn	10.52	3.80
Cl	5.12	2.86
Cu	1.47	0.46

c)

Figure 8. SEM images and EDS analyses after polarization measurements for: a) Cu-Al (position 1), b) the Cu-Al-Ni alloy surface (inside pit) in NaCl solution (position 1), c) the Cu-Al-Mn alloy surface (position 1) in NaCl solution, and d) the Cu-Al-Mn-Ni alloy surface (position 1) in NaCl solution.

Table 4. EDS chemical composition results for corrosion surface layers on copper alloys

Element	Position 2, corrosion product		Position 3, bare metal surface	
	Cu-Al			
	wt.%	at.%	wt.%	at.%
O	48.19	65.01	0.08	0.33
Al	25.62	20.50	0.74	1.72
Cl	20.79	12.66	0.16	0.28
Cu	5.40	1.84	99.02	97.67
	Cu-Al-Ni			
	Position 1		Position 2	
O	2.5	7.9	3.34	10.40
Al	13.18	24.66	12.51	23.10
Cl	0.33	0.46	0.37	0.52
Ni	3.94	3.39	4.11	3.49
Cu	80.04	63.58	79.67	62.49
	Cu-Al-Mn			
	Position 2		Position 3	
O	54.60	72.40	0.28	1.09
Al	19.71	15.50	0.50	1.15
Mn	11.81	4.56	4.07	4.60
Cl	10.98	6.57	0.15	0.26
Cu	2.91	0.97	95.00	92.89
	Cu-Al-Mn-Ni			
	Position 2		Position 3	
O	38.10	57.78	-	-
Al	31.52	21.57	2.10	4.80
Cl	16.76	15.07	-	-
Ni	5.58	2.31	0.98	1.03
Cu	4.51	1.72	96.23	93.39
Mn	3.52	1.55	0.69	0.78

Recent investigations of Nady *et al.* [56] have shown the possibility of forming passive $Ni(OH)_2$ and NiO surface layers in the ternary Cu-Al-Ni alloys in neutral and moderately alkaline solutions, which can further increase resistance of the protective surface layer. EDS analysis showed the presence of Ni on the surface in substantial percentages in all investigated positions.

The SEM image of the Cu-Al-Mn alloy surface shows a more extensively cracked structure of the barrier layer due to polarization treatment. Studies have shown that Mn rapidly diffuses through the alloy, accumulating on grain boundaries and refining the microstructures, leading to improved corrosion resistance, as observed [21,52,56]. The fine microstructure positively affects the compactness and stability of the barrier layer formed on the alloy. Because of the high affinity of Mn towards oxygen, the surface layer on the Cu-Al-Mn alloy contains Mn oxide, as proven by EDS surface analysis. According to the EDS analysis (Figure 8c and Table 4), the top layer (positions 1 and 2) contains high concentrations of O, Al, and Mn (*i.e.* the mixture of Al and Mn oxides) and a smaller amount of Cl and Cu. Further, under the oxide layer, *i.e.* in its cracks (position 3), a large percentage of Cu and lower percentages of Mn, Al, and O are confirmed, while Cl is practically absent. This indicates the naked site of the alloy is covered with a thin oxide layer. Interestingly, the severity and regularity of the cracks on the Cu-Al-Mn alloy surface could be linked to Mn-induced microstructure refinement. Saud and associates reported that Mn addition to Cu-Al-Ni alloy could lead to an 80% reduction in grain sizes, thereby improving the alloys' barrier layer formation and corrosion resistance [21].

According to the literature, the addition of the fourth alloy element in small quantities can improve the mechanical and anti-corrosive properties of alloys

[21,57,58]. For this reason, four-component Cu-Al--Mn-Ni alloys were studied in this paper, as well. The SEM images of the anodically polarized Cu-Al-Mn-Ni alloy (Figures 7 and 8d) show a thick and loose corrosion product layer (as observed for Cu-Al-Ni) that is severely and uniformly damaged (as seen for Cu-Al--Mn). According to EDS analysis, the top layer contains a mixture of Al and Mn oxides, as well as Ni and Cu, while the bare surface below was free of O and Cl, with lower percentages of Al, Ni, and Mn. These results are in complete agreement with results of the corrosion study with Cu-Al-Ni-Mn alloy in 3.5% NaCl solution, performed by Saud *et al.*, confirming that the corrosion products around the damaged areas are rich in Al/Mn oxides and depleted in Cu, while they were dominant on bare metal alloy surfaces with the highest percentage [21].

CONCLUSIONS

- The addition of Al, Ni, and Mn moves the E_{OC} to more positive values.
- Polarization measurements have shown that the alloying element has no significant influence on the copper dissolution mechanism in the Tafel region, where anodic reaction of Cu dissolution was controlled by diffusion of soluble $CuCl_2^-$ in the mass of the solution, (Tafel slope around 60 mV dec^{-1}). The corrosion resistance increases in order: Cu < Cu-Al < Cu--Al-Ni < Cu-Al-Mn < Cu-Al-Mn-Ni. This order was reversed at high anodic potentials, with the Cu alloys displaying higher anodic currents than Cu.
- EIS results indicate that the corrosion resistance of the samples is a consequence of the formation of a barrier layer, whose properties depend on the chemical composition of the alloy, *i.e.*, the type and content of the particular alloying elements. Al, Ni, and Mn have positive effects on barrier layer formation, and the surface film properties become better (higher resistance and thickness, more compact structure).
- SEM/EDS analyses showed that Cu alloys all had thicker and more protective barrier layers, which were severely damaged by extensive anodic polarization. The presence of an oxide layer, consisting of a mixture of dispersing alloying elements, was found on the alloy surfaces.

Acknowledgements

This work was fully supported by the Croatian Science Foundation under project IP-2014-09-3405.

REFERENCES

[1] R. Grecu, A. Samide, G. Eugenia Iacobescu, N. Cioatera, A. Popescu, Chem. Ind. Chem. Eng. Q. 25 (2019) 267--275
[2] V. Grudić, I. Bošković, A. Gezović, Chem. Biochem. Eng. Q. 32 (2018) 299-305
[3] N.D. Nikolić, P.M. Živković, M.G. Pavlović, Z. Baščarević, J. Serb. Chem. Soc. 84 (2019) 1209-1220
[4] J.R. Davis in: Alloying understanding the basics, ASM International, Materials Park, OH, 2004
[5] L. Vrsalović, E. Oguzie, M. Kliškić, S. Gudić, Chem. Eng. Comm. 198 (2011) 1380-1393
[6] R.C.N. Liberto, R. Magnabosco, N. Alonso-Falleiros, Corrosion 63 (2007) 211-219
[7] M.A. Shaik, K.H. Syed, B.R. Golla, Corros. Sci. 153 (2019) 249-257
[8] S. Sathish, U.S. Mallik, T.N. Raju, J. Miner. Mater. Char. Eng. 2 (2014) 71-77
[9] M. Sreekumar, T. Nagarajan Singaperumal, Ind. Robot 34 (2007) 285-294
[10] R. Dasgupta, J. Mater. Res. 29 (2014) 1681-1698
[11] L. Mikova, S. Medvecka-Benova, M. Kelemen, F. Trebuna, I. Virgala, Metalurgija 54 (2015) 169-172
[12] L. Vrsalović, I. Ivanić, S. Kožuh, B. Kosec, M. Bizjak, J. Kovač, U. Gabor and M. Gojić, Corros. Rev. 37 (2019) 579-589
[13] S.N.S. Al-Humairi, Cu-Based shape memory alloys: modified structures and their related properties, Intech open books, 2019, DOI: 10.5772/intechopen.86193
[14] C. Deslouis, B. Tribollet, G. Mengoli, M.M. Musiani, J. Appl. Electrochem. 18 (1988) 374-383
[15] G. Kear, B.D. Barker, F.F. Walsh, Corros. Sci. 46 (2004) 109-135
[16] Y. Van Ingelgem, A. Hubin, J. Vereecken, Electrochim. Acta 52 (2007) 7642-7650
[17] M.M. Antonijević, S.M. Milić, M. B. Petrović, Corros. Sci. 51 (2009) 1228-1237
[18] A.M. Alfantazi, T.M. Ahmed, D. Tromans, Mater. Des. 30 (2009) 2425-2430
[19] H.P. Lee, K. Nobe, J. Electrochem. Soc. 133 (1986) 2035-2043
[20] K.F. Khaled, Mat. Chem. Phys. 125 (2011) 427-433
[21] S.N. Saud, E. Hamzah, T. Abubakar, H. R. Bakhsheshi--Rad, Trans. Nonferrous Met. Soc. China 25 (2015) 1158--1170
[22] M. Gojić, L. Vrsalović, S. Kožuh, A. Kneissl, I. Anžel, S. Gudić, B. Kosec, M. Kliškić, J. Alloys Compd. 509 (2011) 9782-9790
[23] R.G. Blundy, M.J. Pryor, Corros. Sci. 12 (1972) 65-75
[24] H. Shih, H. W. Pickering, J. Electrochem. Soc. 134 (1987) 1949-1957
[25] S. Petetin, J. Crousier, J.P. Crousier, Mater. Chem. Phys. 10 (1984) 317-329
[26] I. Milošev, M. Metikoš Huković, Electrochim. Acta 42 (1997) 1537-1548

[27] I. Milošev, M. Metikoš-Huković, J. Appl. Electrochem. 29 (1999) 393-402

[28] A. Schussler, H.E. Exner, Corros. Sci. 34 (1993) 1803--1811

[29] W.A. Badawy, R.M. El-Sherif, H. Shehata, Electrochim. Acta 54 (2009) 4501-4505

[30] H. Nady, N.H Helal, M.M. Rabiee, WA. Badawy, Mater. Chem. Phys. 134 (2012) 945-950

[31] W. Badawy, M. El-Rabiee, N. Helal, H. Nady, Electrochim. Acta 56 (2010) 913-918

[32] A.O. Moghaddam, M. Ketabchi, R. Bahrami, Trans. Nonferrous Met. Soc. China 23 (2013) 2896−2904

[33] H.H. Kuo, W.H. Wang, Y.F. Hsu, C.A. Huang, Corros. Sci. 48 (2006) 4352-4364

[34] G. Kear, F.C. Walsh, D.B. Barker, K.S. Stokes, EuroCorr 2000, Institute of Corrosion, Leighton Buzzard, 2000

[35] B.A. Boukamp Equivalent Circuit, University of Twente, Twente, 1989

[36] L. Vrsalović, S Gudić, D. Gracić, I. Smoljko, I. Ivanić, M. Kliškić, E. E. Oguzie, Int. J. Electrochem. Sci. 13 (2018) 2102 – 2117

[37] S.N. Saud, E. Hamzah, T. Abubakar, H.R. Bakhsheshi--Rad, Mater. Corr. 66 (2015) 527-534

[38] A.V. Benedetti, P.T.A. Sumodjo, K. Nobe, P.L. Cabot, W. Proud, Electrochim. Acta 40 (1995) 2657-2668

[39] H. Sun, J.E. Orth, H.G. Wheat, JOM 45 (1993) 36-41

[40] M.M. Antonijević, S.C. Alagić, M.B. Petrović, M.B. Radovanović, A.T. Stamenković, Int. J. Electrochem. Sci. 4 (2009) 516-524

[41] A. El Warraky, H.A. El Shayeb, E.M. Sherif, Anti-Corros. Methods 435 Mater. 51 (2004) 52-61

[42] G.C. Serra, A.V. Benedetti, R.D. Noce, J. Braz. Chem. Soc. 8 (2010) 1530-1536

[43] Y.G. Chun, S.I. Pyun, H.C. Kim, Mat. Lett. 20 (1994) 265--270

[44] M. Stern, A.L. Geary. J. Electrochem. Soc. 104 (1957) 56-63

[45] G. Cicileo, B. Rosales, F. Varela, J. Vilche, Corros. Sci. 41 (1999) 1359-1375

[46] D. Zhang, L. Gao, G. Zhou, Appl. Surf. Sci. 225 (2004) 287-293

[47] A. Srivastava, R. Balasubramaniam, Mater. Corros. 56 (2005) 611-618

[48] W.A. Badawy, K.M. Ismail, A.M. Fathi, Electrochim. Acta 50 (2005) 3603-3608

[49] E. Sherif, S.M. Park, Electrochim. Acta 51 (2006) 4665--4673

[50] I.D. Raistrick, J.R. Macdonald, D.R. Franceschetti. in Impedance Spectroscopy, J.R. Macdonald (Ed.), J. Wiley & Sons, New York, 1987

[51] W.A. Badawy, F.M. Al-Kharafi, A.S. El-Azab, Corros. Sci. 41 (1999) 709-727

[52] J.A. Wharton, R.C. Barik, G. Kear, R.J.K. Wood, K.R. Stokes, F.C. Walsh, Corros. Sci. 47 (2005) 3336-3367.

[53] [53] L. Vrsalović, I. Ivanić, S. Kožuh, S. Gudić, B. Kosec, M. Gojić, Trans Nonferrous Met. Soc. China 28 (2018) 1149-1156

[54] D.D. Macdonald, M. Urquidi, J. Electrochem. Soc. 132 (1985) 555-558

[55] D.D. Macdonald, J. Electrochem. Soc. 139 (1992) 3434--3449

[56] H. Nady, M.M. El-Rabiei, M. Samy, W.A. Badawy, J. Bio-Tribo-Corros. 6 (2020) 22

[57] G.N. Sure, L.C. Brown, Metall. Mater. Trans., A 15 (1984) 1613-1621

[58] V. Sampath, Smart Mater. Struct. 14 (2005) S253-S261.

SENKA GUDIĆ[1]
LADISLAV VRSALOVIĆ[1]
ANA RADELJIĆ[1]
EMEKA EMANUEL OGUZIE[2]
IVANA IVANIĆ[3]
STJEPAN KOŽUH[3]
MIRKO GOJIĆ[3]

[1]University of Split, Faculty of Chemistry and Technology, Department of Electrochemistry and Materials Protection, Split, Croatia
[2]Federal University of Technology Owerri, Africa Centre of Excellence in Future Energies and Electrochemical Systems (ACE-FUELS), Owerri, Nigeria
[3]University of Zagreb, Faculty of Metallurgy, Sisak, Croatia

NAUČNI RAD

POREĐENJE KOROZIONOG PONAŠANJA BAKRA I LEGURA BAKRA U HLORIDNOM RASTVORU

Studija poređenja korozionog ponašanja Cu i Cu-Al, Cu-Al-Ni, Cu-Al-Mn i Cu-Al-Mn-Ni u 0,5 mol dm^{-3} NaCl rastvoru sprovedena je merenjem potencijala otvorenog kola, potenciodinamičkom polarizacijom, i merenjem metodom elektrohemijske impedansne spektroskopije (EIS). Skenirajuća elektronska mikroskopija/energetska disperzivna rendgenska spektroskopija (SEM/EDS) korišćena je za procenu korozijonog oštećenja na površini uzoraka nakon polarizacionih merenja. Dobijeni rezultati ukazuju da legirani elementi dovode do smanjenja gustine katodne i anodne struje u Tafelovom području, povećanja anodne struje pri višim anodnim potencijalima i blagog pozitiviranja korozionog potencijala. Sveukupno, impedancija raste sledećim redosledom: Cu < Cu-Al < Cu-Al--Ni < Cu-Al-Mn < Cu-Al-Mn-Ni. Ovo ukazuje na to da Cu legure imaju bolju otpornost na koroziju. SEM snimci površine uzoraka i EDS analiza nakon polarizacionih merenja pokazuju jednolično rastvaranje čistog Cu, kao i prisutnost površinskog oksidnog sloja, sastavljenog od oksida odgovarajućih legirajućih elemenata, na površini ispitivanih legura. Destruktivna anodna polarizacija dovodi do značajnih oštećenja barijernih slojeva na uzorcima legura.

Ključne reči: legure bakra, korozija, elektrohemijske metode, polarizacija, legure sa memorijom oblika, SEM/EDS.